Kinetic-inductance-limited reset time of superconducting nanowire photon counters

Andrew J. Kerman,[a] Eric A. Dauler, and William E. Keicher
Lincoln Laboratory, Massachusetts Institute of Technology, Lexington, Massachusetts 02420

Joel K. W. Yang and Karl K. Berggren
Research Laboratory of Electronics, Massachusetts Institute of Technology, Cambridge, Massachusetts 02139

G. Gol'tsman and B. Voronov
Moscow State Pedagogical University, Moscow 119345, Russia

We investigate the recovery of superconducting NbN-nanowire photon counters after detection of an optical pulse at a wavelength of 1550 nm, and present a model that quantitatively accounts for our observations. The reset time is found to be limited by the large kinetic inductance of these nanowires, which forces a tradeoff between counting rate and either detection efficiency or active area. Devices of usable size and high detection efficiency are found to have reset times orders of magnitude longer than their intrinsic photoresponse time. © *2006 American Institute of Physics.*
[DOI: 10.1063/1.2183810]

High-speed photon-counting detectors have many applications, including optical communications,[1] quantum information,[2] semiconductor processing,[3] and laser radar.[4] Of particular interest would be a detector that exhibits both ultrafast count rates ($\geq$GHz) and high single-photon detection efficiency at near-infrared wavelengths ($\sim$1550 nm); however, this combination is not available with current technologies. InGaAs avalanche photodiodes are limited to much lower count rates by long reset times[5] and hybrid photomultipliers have low detection efficiencies at these wavelengths.[6]

A promising detector technology was reported recently, in which superconducting NbN nanowires are biased with a dc current I_{bias} slightly below the critical value I_C.[7] An incident photon of sufficient energy can produce a resistive "hotspot" which in turn disrupts the superconductivity across the wire, resulting in a voltage pulse. Observations of this photoresponse showed promise for high counting rates, with measured intrinsic response times as low as $\sim$30 ps,[8] and counting rates in the GHz regime.[9,10] In this letter, we present our own investigation into the counting-rate limitation of these devices, in which we directly observe the recovery of the detection efficiency as the device resets (after a detection event), and develop a quantitative model of this process. We find that detectors having both high detection efficiency and usable active area are limited to much lower count rates than studies of their intrinsic response time had suggested.[8]

We fabricated our nanowires using a newly developed process,[11] on ultrathin (3–5 nm) NbN films.[12] We used several geometries, including straight nanowires having widths from 20–400 nm and lengths from 0.5–50 μm, as well as large-area "meander" structures[9,10] [e.g., Fig. 1(b)] having active-area aspect ratios from 1–50, fill factors from 25–50%, and sizes up to 10 μm square. The devices had critical temperatures $T_C \sim 9$–10 K, and critical current densities $J_C \sim 2$–5×10^{10} A/m^2. In total, $\sim$400 devices were tested, spanning several different fabrication runs.

The devices were cooled to as low as 2 K inside a cryogenic probing station (Desert Cryogenics), as illustrated in Fig. 1(a). Electrical contact was established using a cooled 50 Ω microwave probe attached to a micromanipulator, and connected via coaxial cable to the room-temperature electronics. Current was supplied through the dc port of a bias T using a battery-powered adjustable voltage source in series with a 100 kΩ resistor. The ac port of the bias T was connected through a 3 dB attenuator to a low-noise amplifier, and then through a dc block to a 6 GHz real-time oscilloscope, pulse counter, and a fast flip-flop as described below. To optically probe the devices, we used a 1550 nm mode-locked fiber laser, with a 10 MHz pulse repetition rate and $\leq$1 ps pulse duration, that was sent through an attenuator and polarization controller and then into the probing station via an optical fiber. The devices were illuminated through a lens attached to the end of the fiber and mounted to a second micromanipulator, at an incidence angle of $\sim$15° (from normal to the sample surface). The focal spot had a measured e^{-2} radius of $\sim$8 μm. Figures 2(a)–2(d) show output pulses for 100 nm wide wires with total lengths from 5–500 μm.

The microscopic mechanism for the formation and growth of a resistive hotspot after photon absorption has been discussed by other authors.[13] Here, we use a simple phenomenological model, illustrated in Fig. 2(e). A central feature of this model is the kinetic inductance of the wire L_k, which can be much larger than the geometric (magnetic) inductance for thin films.[14,15] Absorption of a photon corresponds to the switch opening, at which time the wire acquires a resistance R_n.[16] The current in the device then begins to decay from its initial value I_{bias} with a time constant $\tau_{\text{fall}} = L_k / [50 \, \Omega + R_n]$, toward a final value $I_n = I_{\text{bias}} \times 50 \, \Omega / [50 \, \Omega + R_n]$. This decay is interrupted, however, at some "return" current I_{ret} when the self-heating of the wire, given by $I(t)^2 R_n$, is sufficiently reduced that the wire becomes fully superconducting again.[14] The switch in our model then closes, and the current recovers to its original value with the time constant $\tau_{\text{rise}} = L_k / 50 \, \Omega$.[17] From the observed asymmetry of the electrical pulses ($\tau_{\text{fall}} \ll \tau_{\text{rise}}$),[18] we conclude that $R_n \geq 50 \, \Omega$; in this limit, the pulse amplitude
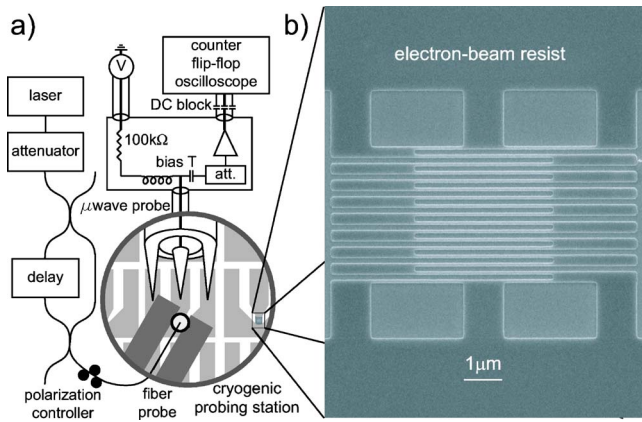
a)Electronic mail: ajkerman@ll.mit.edu

FIG. 1. (Color online) Schematic of the experimental setup. (a) A cryogenic probing station allowed us to probe our devices both electrically and optically. Our samples were 3–8 mm in size, and typically contained from 50–150 individual, separately addressable detectors. (b) A scanning electron microscope image of the electron-beam resist pattern used to define a large-area meander structure.[9,10]

FIG. 2. (Color online) Inductance-limited recovery of NbN nanowires. Output pulses are shown for 100 nm wide wires at $T=4.2$ K, with I_{bias} =11.5 μA, and dimensions: (a) 10 μm × 10 μm meander (total length 500 μm); (b) 4 μm × 6 μm (120 μm); (c) 3 μm × 3.3 μm (50 μm); and (d) 5 μm long single wire. Red dotted lines show the predicted pulse recovery, with no free parameters, for each device based on its measured inductance: L_k=415 nH, 110 nH, 44.5 nH, and 6.10 nH. These predictions include the effect of the measured f_L=15 MHz and f_H=4 GHz corner frequencies of our amplifiers, and the assumptions: $I_{ret} \ll I_{bias}$, $R_n \gg 2\pi f_H L_k$, and $R_n \gg 50$ Ω (the pulse risetime is then determined by f_H); and (e) electrical model; photon absorption corresponds to the switch opening, after which the detector current goes nearly to zero, and is diverted into the 50 Ω load. The wire then becomes superconducting again, and the current resets in a time τ_{rise}. (f) Inductance at $T=4.2$ K vs room-temperature resistance for 290 individual nanowires from 0.5–500 μm long and 20–400 nm wide, with both straight and meander geometries, from two separate samples made in separate fabrication runs. Points corresponding to the devices of (a)–(d) are indicated. The slope of a linear fit constrained to pass through the origin, shown by a solid line, is 0.997±0.002; this indicates that $L \propto R_{300K}$, and therefore that L is predominantly a kinetic inductance.

reduces to: $V_{pulse} \approx (I_{bias} - I_{ret}) \times 50$ $\Omega \times G_{sig}$, where G_{sig} =47.8 dB is the measured total gain of our signal path in the amplifier passband. Since the observed pulse amplitudes for all devices were well described by $V_{pulse} \approx I_{bias} \times 50$ $\Omega \times G_{sig}$, we conclude that $I_{ret} \ll I_{bias}$. The kinetic inductance L_k, which determines the current recovery time, was measured for each of our devices using a network analyzer. The dashed red lines shown in Figs. 2(a)–2(d) are the resulting pulse shapes predicted by our model with no free parameters.

To verify that the large observed inductances were indeed primarily kinetic in nature, we compared them to the corresponding room-temperature resistances R_{300K}. Kinetic inductance should be proportional to R_{300K}, since both have the same dependence on wire geometry: $R_{300K} = \mathcal{R}_{300K} \int ds/A(s)$ and $L_k = \mathcal{L}_k \int ds/A(s)$, where $\mathcal{R}_{300K}$ and $\mathcal{L}_k$ are the resistivity and kinetic inductivity, A is the cross-sectional area, and integration is along the wire. This proportionality is demonstrated in Fig. 2(f) for 290 different devices spanning nearly three decades of inductance.[19]

To optically probe each device, we aligned the fiber probe with it by maximizing its electrical output pulse rate as observed on the pulse counter. Varying the polarization of the light produced up to a factor of 2 change in the count rate, and we chose the polarization that maximized this rate. Using the calibration procedure reported in Ref. 20 we measured a single-photon detection efficiency at $T=4.2$ K and $I_{bias}=0.98 I_C$ of 2.8% for the 4 μm × 6 μm meander device with 100 nm wire width and 50% fill factor used in the experiments described below (this device had $I_C \approx 15$ μA at 4.2 K).

To investigate the time-dependence of the detection efficiency after a detection event, we illuminated the devices with optical pulse pairs,[9] and measured the probability that *both* pulses were detected, as a function of the pulse separation. As shown in Fig. 1, we split the output of our laser into two components, one of which passed through a 0–15 ns optical delay line. The two components were then recombined to produce pulse pairs with controllable separation. The output of the amplifiers was sent to a flip-flop, which switches its digital state every time it is triggered. We then used the oscilloscope to count only those digital pulses from the flip-flop having a width nearly equal to the optical pulse
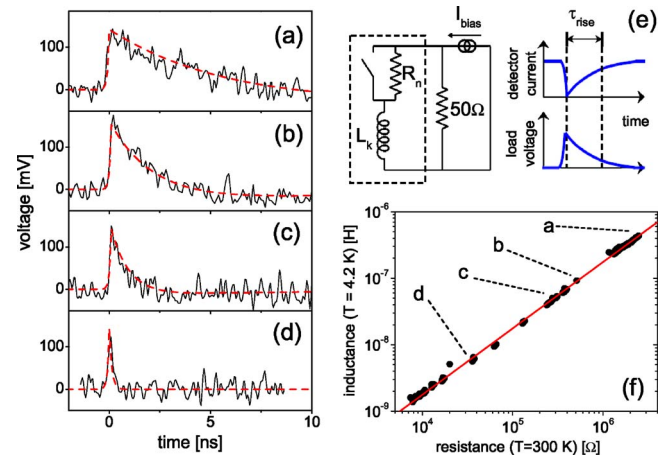
separation, from which we obtained the probability that the device detected both optical pulses in a pair. The result is shown in Fig. 3 for two different devices, with each scaled to its asymptotic value.[21] The solid lines are the predictions of our model for the two devices, with no free parameters. Figures 3(b) and 3(c) illustrate how these curves were generated. For a given time on the abscissa of (a), we first found the
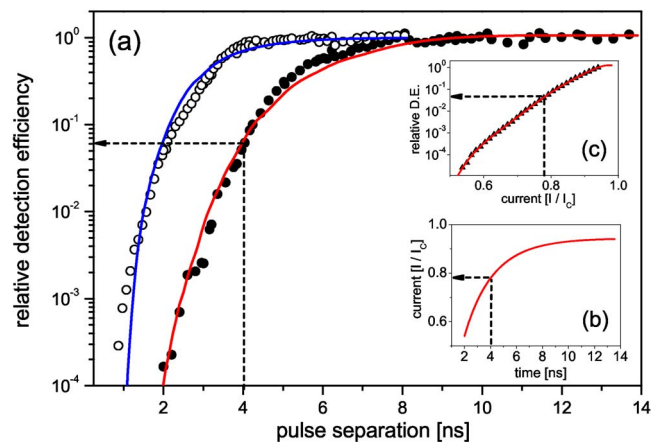

FIG. 3. (Color online) Recovery of the detection efficiency after a detection event. (a) Filled circles are data obtained with a 4 μm × 6 μm meander with 100 nm wide wire and a 50% fill factor, open circles indicate a device of the same size but with a 25% fill factor. Solid curves are the predictions of our model with no free parameters, obtained as illustrated in (b) and (c) for the 50% fill device, based on the measured inductances[22] [109 nH and 47.1 nH at $I_{bias}=0$] and detection efficiency vs I_{bias} curves.

instantaneous current predicted by our model, based on the measured inductance,[22] as shown in (b). The current was assumed to start at zero (based on our earlier conclusion that $I_{ret} \ll I_{bias}$).[23] The current at each time point was then mapped to a relative detection efficiency (RDE) value using a polynomial fit to the measured detection efficiency versus I_{bias}, shown in (c). An example of this mapping is illustrated by the dotted arrows, with $t=4$ ns $\rightarrow I/I_C = 0.78 \rightarrow$ RDE $= 6 \times 10^{-2}$. The resulting predictions agree well with our data for these two devices, which have very different inductances, supporting our model of the reset process in these nanowires.

Figure 3 has important implications for high-speed applications of these devices. For the 50% fill device, it took 8.5 ns for the detection efficiency to recover to 90% of its initial value, and the device will therefore not support counting rates $\gtrsim 120$ MHz near full detection efficiency. Although much higher counting rates can readily be achieved with lower-inductance devices, reducing the inductance presently requires either reducing the device area, increasing the wire width, or increasing the film thickness (which explain the GHz counting rates observed in Ref. 9), any of which would reduce the system detection efficiency.

As a final note, although our model and conclusions are fully consistent with the observations in Refs. 9 and 24 they contradict those presented in Ref. 10, where both high detection efficiencies and GHz counting rates were reported for the same 10 μm square device. We and the NIST group[24] have both independently tested nominally identical devices to this one, fabricated by the Moscow group using the same process and with the same dimensions as those used in Ref. 10, and have observed pulse shapes consistent with the conclusions of the present work. However, the discrepancy might have arisen from some difference in the measurement apparatus used.

In summary, we have shown that the reset time of superconducting NbN-nanowire photon counters is limited by the large kinetic inductance inherent in any thin superconducting film. This result implies that present devices with usable active area and high detection efficiency are intrinsically limited to counting rates well below the GHz regime suggested by early measurements,[8] and that any future attempts to increase the counting rates accessible to these devices will have to circumvent their large kinetic inductance. If this can be achieved, the full potential of these devices may become accessible: With an intrinsic photoresponse time as short as ~ 30 ps,[8] they could extend photon counting into the tens of GHz regime characteristic of modern telecommunications.

[1]R. M. Gagliardi and S. Karp, *Optical Communications* (Wiley, New York, 1976); J. R. Pierce, IEEE Trans. Commun. **26**, 1819 (1978).

[2]N. Gisin, G. G. Ribordy, W. Tittel, and H. Zbinden, Rev. Mod. Phys. **74**, 145 (2002); E. Knill, R. Laflamme, and G. J. Milburn, Nature (London) **409**, 46 (2001).

[3]J. A. Kash and J. C. Tsang, Phys. Status Solidi B **204**, 507 (1997).

[4]W. C. Priedhorsky, R. C. Smith, and C. Ho, Appl. Opt. **35**, 441 (1996).

[5]P. L. Voss, K. G. Köprülü, S.-K. Choi, S. Dugan, and P. Kumar, J. Mod. Opt. **51**, 1369 (2004).

[6]R. A. La Rue, K. A. Costello, C. A. Davis, J. P. Edgecumbe, and V. W. Aebi, IEEE Trans. Electron Devices **44**, 672 (1997).

[7]A. M. Kadin and M. W. Johnson, Appl. Phys. Lett. **69**, 3938 (1996); G. Goltsman, O. Okunev, G. Chulkova, A. Lipatov, A. Dzardanov, K. Smirnov, A. Semenov, B. Voronov, C. Williams, and R. Sobolewski, IEEE Trans. Appl. Supercond. **11**, 574 (2001).

[8]K. S. Il'in, M. Lindgren, M. Currie, A. D. Semenov, G. N. Gol'tsman, R. Sobolewski, S. I. Cherednichenko, and E. M. Gershenzon, Appl. Phys. Lett. **76**, 2752 (2000).

[9]J. Zhang, W. Slysz, A. Verevkin, O. Okunev, G. Chulkova, A. Korneev, A. Lipatov, G. N. Gol'tsman, and R. Sobolewski, IEEE Trans. Appl. Supercond. **13**, 180 (2003).

[10]A. Pearlman, A. Cross, W. Slysz, J. Zhang, A. Verevkin, M. Currie, A. Korneev, P. Kouminov, K. Smirnov, B. Voronov, G. Gol'tsman, and R. Sobolewski, IEEE Trans. Appl. Supercond. **15**, 579 (2005).

[11]The process followed the description given in J. K. W. Yang, E. Dauler, A. Ferri, A. Pearlman, A. Verevkin, G. Gol'tsman, B. Voronov, R. Sobolewski, W. E. Keicher, and K. K. Berggren, IEEE Trans. Appl. Supercond. **15**, 626 (2005), with the following notable modifications: only the hydrogen silsesquioxane process with a resist thickness of 100 nm was used; the resist was developed for 8 min; and reactive-ion etching was uninterrupted (2 min at 20 mTorr and 116 V dc self-bias).

[12]S. Cherednichenko, P. Yagoubov, K. Il'in, G. Gol'tsman, and E. Gershenzon, in *Proceedings of the 8th International Symposium On Space Terahertz Technology*, Boston, MA, 1997, p. 245.

[13]A. Semenov, G. Gol'tsman, and A. Korneev, Physica C **351**, 349 (2001).

[14]See, for example, A. M. Kadin, *Introduction to Superconducting Circuits* (Wiley, New York, 1999).

[15]M. W. Johnson and A. M. Kadin, IEEE Trans. Appl. Supercond. **7**, 3492 (1997).

[16]We assumed that the inductance was unaffected by the presence of R_n (i.e., the normal domain covered only a small fraction of the wire).

[17]In reality, $I(t)$ and $R(t)$ interact dynamically through Joule heating $I(t)^2 R(t)$. Our simplified model approximates this time-dependent $R(t)$ with a square pulse of height R_n, lasting from the photon absorption at $t=0$ to the time when $I(t)=I_{ret}$.

[18]The 4 GHz bandwidth of our amplifiers obscured the asymmetry of the pulses from very short wires.

[19]From these data, we can extract the magnetic penetration depth λ, using: $\mathcal{L}_k \approx \mu_0 \lambda^2$ (valid in the limit $\lambda \gg t$ where t is the film thickness). Assuming $t=4$ nm, we obtain from the inductance data: $\langle \mathcal{L}_k \rangle = 360$ pH nm and $\langle \lambda \rangle = 535$ nm (brackets indicate an average over devices).

[20]K. M. Rosfjord, J. K. W. Yang, E. A. Dauler, A. J. Kerman, V. Anant, B. M. Voronov, G. N. Gol'tsman, and K. K. Berggren, Opt. Express **14**, 527 (2006).

[21]In order to acquire detection efficiencies over a wide dynamic range in a reasonable time, a relatively high optical intensity was used for these pulse-pair measurements, corresponding to an individual (isolated) pulse detection probability $P_p \sim 0.57$ for both devices (or $N \sim 70$ and $N \sim 220$ photons per pulse incident on the active areas of the 50% and 25% fill factor devices, respectively). Measured values of P_p were converted to single-photon detection efficiency $P_{1\gamma}$ using the relation: $P_p = 1 - \exp(-N P_{1\gamma})$.

[22]The inductance was also measured as a function of I_{bias}, and was observed to increase by up to 10% close to I_C. This was included numerically in our model.

[23]A small time offset was added to each prediction, to account for the time it took the current to decay to zero and the device to return to the superconducting state. These offsets were fixed at the observed fall times of the electrical pulses for each device, 330 and 160 ps for the 50% and 25% fill devices, respectively.

[24]R. H. Hadfield, A. J. Miller, S. W. Nam, R. L. Kautz, and R. E. Schwall, Appl. Phys. Lett. **87**, 203505 (2005).